



Radiomics improves efficiency for differentiating subclinical pheochromocytoma from lipid-poor adenoma: a predictive, preventive and personalized medical approach in adrenal incidentalomas

Xiaoping Yi^{1,2} · Xiao Guan³ · Youming Zhang¹ · Longfei Liu³ · Xueying Long¹ · Hongling Yin⁴ · Zhongjie Wang⁵ · Xuejun Li⁵ · Weihua Liao¹ · Bihong T. Chen⁶ · Chishing Zee⁷

Received: 3 July 2018 / Accepted: 30 August 2018 / Published online: 21 September 2018
© European Association for Predictive, Preventive and Personalised Medicine (EPMA) 2018

Abstract

Objectives This study aims to define a radiomic signature for pre-operative differentiation between subclinical pheochromocytoma (sPHEO) and lipid-poor adrenal adenoma (LPA) in adrenal incidentaloma. The goal was to apply a predictive, preventive, and personalized medical approach to the management of adrenal tumors.

Patients and methods This retrospective study consisted of 265 consecutive patients (training cohort, 212 (LPA, 145; sPHEO, 67); validation cohort, 53 (LPA, 36; sPHEO, 17)). Computed tomography (CT) imaging features were evaluated, including long diameter (LD), short diameter (SD), pre-enhanced CT value (CT_{pre}), enhanced CT value (CT_{post}), shape, homogeneity, necrosis or cystic degeneration (N/C). Radiomic features were extracted and then were used to construct a radiomic signature (Rad-score) and radiomic nomogram. The area under the receiver operating characteristic curve (AUC) was used to evaluate their performance.

Results Sixteen of three hundred forty candidate features were used to build a radiomic signature. The signature was significantly different between the sPHEO and LPA groups (AUC: training, 0.907; validation, 0.902). The radiomic nomogram based on enhanced CT features (M1) consisted of Rad-score, LD, SD, CT_{pre}, shape, homogeneity and N/C (AUC: training, 0.957; validation, 0.967). The pre-enhanced CT features based radiomic nomogram (M2) included Rad-score, LD, SD, CT_{pre}, shape, and homogeneity (AUC: training, 0.955; validation, 0.958).

Conclusions Our radiomic nomograms based on pre-enhanced and enhanced CT images distinguished sPHEO from LPA. In addition, the promising result using pre-enhanced CT images for predictive diagnostics is important because patients could avoid the additional radiation and risk associated with enhanced CT.

Keywords Adrenal gland neoplasms · Pheochromocytoma · Adrenal adenoma · Predictive preventive personalized medicine · Computed tomography · Radiomics

Xiaoping Yi and Xiao Guan contributed equally to this work.

Electronic supplementary material The online version of this article (<https://doi.org/10.1007/s13167-018-0149-3>) contains supplementary material, which is available to authorized users.

✉ Xiaoping Yi
yixiaoping@csu.edu.cn

✉ Youming Zhang
zhangym0820@csu.edu.cn

¹ Department of Radiology, Xiangya Hospital, Central South University, No. 87 Xiangya Road, Changsha 410008, People's Republic of China

² Postdoctoral Research Workstation of Pathology and Pathophysiology, Basic Medical Sciences, Xiangya Hospital, Central South University, Changsha, China

³ Department of Urology, Xiangya Hospital, Central South University, Changsha, China

⁴ Department of Pathology, Xiangya Hospital, Central South University, Changsha, China

⁵ Department of Neurosurgery, Xiangya Hospital, Central South University, Changsha, China

⁶ Department of Diagnostic Radiology, City of Hope National Medical Centre, Duarte, CA, USA

⁷ Department of Radiology, Keck Medical Center of USC, Los Angeles, CA, USA

Abbreviations

AA	Adrenal adenoma
AI	Adrenal incidentaloma
AUC	Area under the receiver operating characteristic curve
CT	Computed tomography
CT _{pre}	Pre-enhanced CT value
CT _{post}	Enhanced CT value
ICC	Intraclass correlation coefficient
LASSO	Least absolute shrinkage and selection operator
LD	Long diameter
LPA	Lipid-poor adrenal adenoma
MRI	Magnetic resonance imaging
N/C	Necrosis or cystic degeneration
PET	Positron emission tomography
sPHEO	Subclinical pheochromocytoma
ROC	Receiver operating characteristic
SD	Short diameter

Introduction

In recent years, predictive, preventive, and personalized medicine (PPPM) has been advocated in the field of tumor research and has become the direction of future research [1]. It is evident that a paradigm shift in medicine is needed to move from traditional reactive medical practice to PPPM to devise treatment strategies [1–3]. Applying PPPM to the clinical management of adrenal incidentalomas (AIs), it is important to predict the pathology of the adrenal tumors before surgery to prevent perioperative morbidity and mortality. A subclinical pheochromocytoma (sPHEO) may pre-dispose the patient to life-threatening hypertensive crises during surgery, which may lead to serious cardiovascular events. However, due to the overlap in imaging features and non-specific clinical findings, sPHEO is frequently misdiagnosed as other AIs, such as lipid-poor adrenal adenoma (LPA) [4–9]. There has been no clear way to distinguish sPHEO and LPA based on traditional radiological analysis. New imaging-related methodologies with a PPPM approach might be useful to improve predictive diagnosis for AI.

Radiomics is a PPPM-based approach that uses computerized quantitative imaging analysis for extracting large numbers of image-related features, such as intensity, geometry, and texture, from medical images [10]. In short, radiomics converts medical images into numerical values that could not be obtained by observation of the image. This process uses high-throughput data-extraction algorithms, which enable subsequent data analysis and model building [11–13]. Recent radiomic studies have shown promising results for tumor differentiation and subtype classification [14, 15]. This method provides an alternative to traditional imaging analysis, and it may assist in the development of predictive diagnostics for

personalized medicine [16–18]. However, the effectiveness of a radiomic approach in differentiating sPHEO from LPA is not known.

In the present study, we retrospectively evaluated 265 cases that had been surgically resected with pathological confirmation of sPHEO and LPA. We developed radiomic nomograms and validated their efficiency for differentiating between sPHEO and LPA.

Materials and methods

Patients

This retrospective study was approved by the Ethics Committee and Institutional Review Board in Xiangya Hospital of Central South University, P. R. China (IRB No. 201612638). Informed consent was waived for all patients.

Data for surgically and pathologically confirmed adrenal adenoma (AA) and pheochromocytoma cases in our hospital were collected from 1 June 2006 to 31 December 2017 using a search of our institutional database and medical record system. None of the patients included in this study received tumor-related therapy before the computed tomography (CT) scans. Patients without detailed medical records, pathological results, or quality pre-operative CT images were excluded. The patients included in this study were divided into two cohorts (training and validation) at a ratio of 4:1 using computer-generated random numbers. This process is shown in Fig. 1. Enhanced CT (CT_{post}) features and pre-enhanced (CT_{pre}) features were used to generate the radiomic nomograms M1 and M2, respectively.

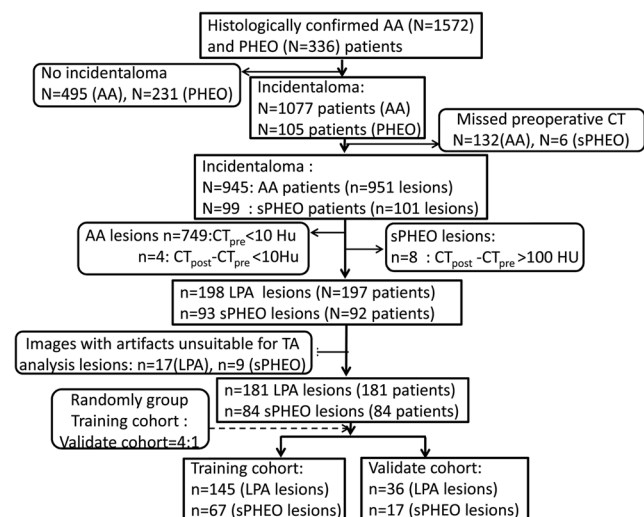


Fig. 1 The patient recruitment pathway, along with the inclusion and exclusion criteria. Note: *PHEO*, pheochromocytoma; *AA*, adrenal adenoma; *sPHEO*, subclinical pheochromocytoma; *LPA*, lipid-poor adenoma; *CT_{pre}*, pre-enhanced CT value (Hu); *CT_{post}*, enhanced CT value (Hu)

CT image acquisition, retrieval, analysis, and feature extraction

Details about CT image acquisition, retrieval, and analysis, as well as the algorithms for radiomic feature extraction [19] are in the Electronic supplementary material, along with intraobserver (two observations by reader 1) and interobserver (reader 1 vs. reader 2) reproducibility evaluation methods.

Radiomic feature selection and signature building

The least absolute shrinkage and selection operator (LASSO) method, which is suitable for analyzing large sets of radiomic features and regression of high-dimensional data, was applied to select the most significant predictive feature from the training cohort. Most of the coefficients of the covariates were reduced to zero, and the remaining non-zero coefficients were selected by LASSO. The non-zero coefficients of the selected features were used to construct the radiomic signature (Rad-score). The Rad-score was calculated for each patient via a linear combination of selected features that were weighted by their respective coefficients.

Diagnostic validation of the radiomic signature

The potential use of the Rad-scores to differentiate the two lesions was first evaluated in the training cohort and then in the validation cohort using the area under the receiver operating characteristic (ROC) curve (AUC).

Development and performance of a radiomic nomogram based on enhanced CT images

Multivariable logistic regression analysis was performed with both the Rad-scores and the CT imaging features showing significant differences between sPHEO and LPA patients. A radiomic signature was applied to build a predictive model for differentiating sPHEO from LPA using the training cohort.

To provide the clinicians with a quantitative tool for accurate diagnosis, we built a nomogram (M1) using multivariable logistic regression analysis of CT_{post} images in the training cohort. AUC analysis was used to quantify the predictive performance of the radiomics nomogram in the training cohort. The AUC values were then used to test the predictive performance of the radiomics nomogram in the validation cohort. A calibration curve was obtained from multivariable Cox proportional hazard regression analysis.

Development and performance of a radiomics nomogram without enhanced CT features

To evaluate the feasibility and efficiency of the radiomic nomogram using non-enhanced CT images in the classification

task, another radiomic nomogram (M2) was developed for the CT_{pre} imaging features using the training cohort. The predictive performance of the M2 model was validated in the validation cohort using AUC values. A calibration curve was obtained from multivariable Cox proportional hazard regression analyses.

Statistical analysis

Quantitative data with a normal distribution are presented as the mean \pm SD, and the groups were compared using an independent Student's *t* test. Quantitative data with a non-normal distribution are presented as medians (interquartile ranges), and the groups were compared using a Wilcoxon rank sum test. Patient sex ratios and lesion location ratios between the two groups were compared using a chi-square test. The LASSO regression was performed using MATLAB. Other statistical analyses were performed using R software. A two-sided *P* value was computed, and statistical significance was set at 0.05.

Results

Clinical characteristics of the patients

The patient characteristics for the training and validation cohorts are summarized in Table 1. There were no significant differences in the clinical characteristics between the training cohort and validation cohort, for either the sPHEO or LPA group, which justified their use as training and validation cohorts.

Inter- and intraobserver reproducibility of radiomic feature extraction

Satisfactory inter- and intraobserver reproducibility of the texture feature extraction was achieved. The interobserver intraclass correlation coefficients (ICCs) calculated based on features extracted by reader 1 (first extraction) and reader 2 ranged from 0.775 to 0.907. The intraobserver ICCs, calculated based on reader 1's feature extraction results from two attempts, ranged from 0.794 to 0.933. Therefore, all outcomes were based on the features extracted by reader 1.

Radiomic feature extraction and radiomic signature construction

A total of 340 features were extracted from the unenhanced CT images. Figure S1 contains a visual representation of the extracted radiomic features of all the patients. From this representation, an estimated classification was visible based on

Table 1 Characteristics of patients in the training and validation cohorts

Characteristic	Training cohort		<i>P</i> value	Validation cohort		<i>P</i> value
	sPHEO	FA		sPHEO	FA	
Gender (No. (%))						
Male	28 (41.79)	81 (55.86)	< 0.001	7 (41.18)	22 (61.11)	< 0.001
Female	39 (58.21)	64 (44.14)		10 (58.82)	14 (38.89)	
Age (mean ± SD, years)	47.8 ± 13.1	46.3 ± 12.5	0.262	46.4 ± 12.7	47.6 ± 10.2	0.804
LD (mm) (median (interquartile range))	52.0 (39.0–68.0)	22.0 (15.5–32.0)	< 0.001	46.0 (34.5–59.0)	21.5 (17.3–30.8)	< 0.001
SD (mm) (median (interquartile range))	43.0 (32.0–56.0)	18.0 (11.0–27.0)	< 0.001	37.0 (30.0–51.0)	18.0 (12.0–26.5)	< 0.001
CT _{pre} (Hu) (median (interquartile range))	35.4 (30.9–42.0)	22.0 (16.0–31.5)	< 0.001	37.0 (30.5–40.0)	19.5 (15.3–30.0)	< 0.001
Shape						
Regular	40 (59.70)	118 (81.38)	< 0.001	7 (41.18)	26 (72.22)	0.03
Irregular	27 (40.30)	27 (18.62)		10 (58.82)	10 (27.78)	
Homogeneity						
Homogenous	9 (13.43)	103 (71.03)	< 0.001	4 (23.53)	27 (36.00)	< 0.001
Heterogenous	58 (86.57)	42 (28.97)		13 (76.47)	9 (64.00)	
Necrosis						
No	18 (26.87)	131 (90.34)	< 0.001	4 (23.53)	34 (94.44)	< 0.001 ^a
Yes	49 (73.13)	14 (9.66)		13 (76.47)	2 (5.56)	
Calcification						
No	64 (95.52)	140 (96.55)	0.710	16 (94.12)	36 (100)	0.321 ^a
Yes	3 (4.48)	5 (3.45)		1 (5.88)	0 (0)	
Counter						
Sharp	1 (1.49)	4 (2.76)	0.677 ^a	2 (11.76)	0 (0)	0.099 ^a
Blotted	66 (98.51)	141 (97.24)		15 (88.24)	36 (100)	
Rad-score (median (interquartile range))	0.4315 (0.2939–0.5469)	0.8311 (0.6908–0.9176)	< 0.001	0.4717 (0.3586–0.5759)	0.7976 (0.6959–0.9330)	< 0.001

Note: *P* value is derived from the univariable association analyses between each of the clinicopathologic variables and LN status

Abbreviations: *SD*, standard deviation; *LD*, long diameter; *SD*, short diameter; *CT_{pre}*, pre-enhanced CT values; *Rad-score*, radiomics score

**p* < 0.05

^a Fisher's exact test

the differences in texture associated with the two diagnoses. Of these features, 16 were selected by LASSO for inclusion (Fig. S1) in the Rad-score calculation formula, as shown in the Electronic supplementary material.

Figure S2 contains a graphical presentation of the Rad-scores for the patients in the training and validation cohorts. The patients' diagnoses were represented by the color-coding scheme, and the Rad-score values were sorted in ascending order, a clear classification of LPA and sPHEO images could be observed.

Diagnostic validation of the radiomic signature

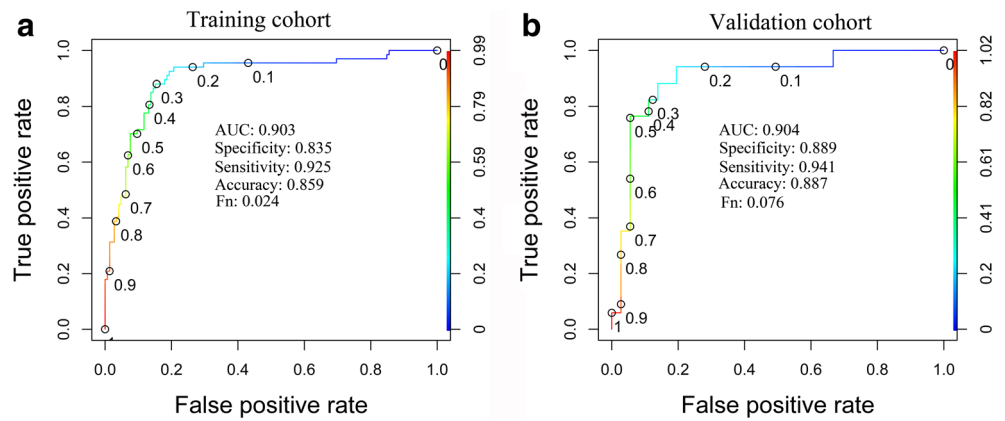
A significant difference was found in the Rad-scores between sPHEO and LPA patients in the training cohort (*P* < 0.001), which was further confirmed in the validation cohort. Patients with sPHEO generally had higher Rad-scores in the training

cohort. The radiomic signature yielded an AUC of 0.903 in the training cohort and 0.904 in the validation cohort. A Rad-score value of more than 0.661 was considered sPHEO, with a sensitivity of 92.5% and specificity of 83.5%. ROC curves are presented in Fig. 2.

Development of a radiomic nomogram

Multivariable logistic regression analysis was performed with Rad-score, LD, SD, CT_{pre}, shape, homogeneity, and N/C. A prediction model incorporating the above predictors was developed and is presented as a nomogram in Fig. 3. This model (M1) provided an AUC of 0.957 in the training cohort and 0.967 in the validation cohort (Fig. 3). An M1 value of more than 75.97 could be diagnosed as sPHEO, with a sensitivity of 89.7% and specificity of 95.5%.

Fig. 2 Receiver operating characteristic (ROC) curve analysis based on the radiomic signature (Rad-score). Cut-off values are indicated along the curves. **a** ROC curve of the training cohort. **b** ROC curve of the validation cohort. *F_n*, false-negative rate



Development of a radiomic nomogram without enhanced CT features

To determine whether pre-enhanced CT images were sufficient to distinguish sPHEO from LPA, the M2 nomogram was constructed without inclusion of the imaging features from the enhanced CT. M2, which was developed without N/C, also showed a promising AUC of 0.955 in the training cohort and 0.958 in the validation cohort. These were very

close to the values obtained when N/C was included. The corresponding ROC curves are shown in Fig. 4. A M2 value of more than 81.50 could be diagnosed as sPHEO, with a sensitivity of 97.0% and specificity of 84.8%.

Validation of the radiomic nomogram

The calibration curves for the two radiomic nomograms to be used for differentiation between sPHEO and LPA, based on

Fig. 3 The receiver operating characteristic (ROC) curves and the corresponding nomogram with multiple predictors. Cut-off values are indicated along the curves. **a** ROC curve for the training cohort. **b** ROC curve for the validation cohort. **c** Nomogram

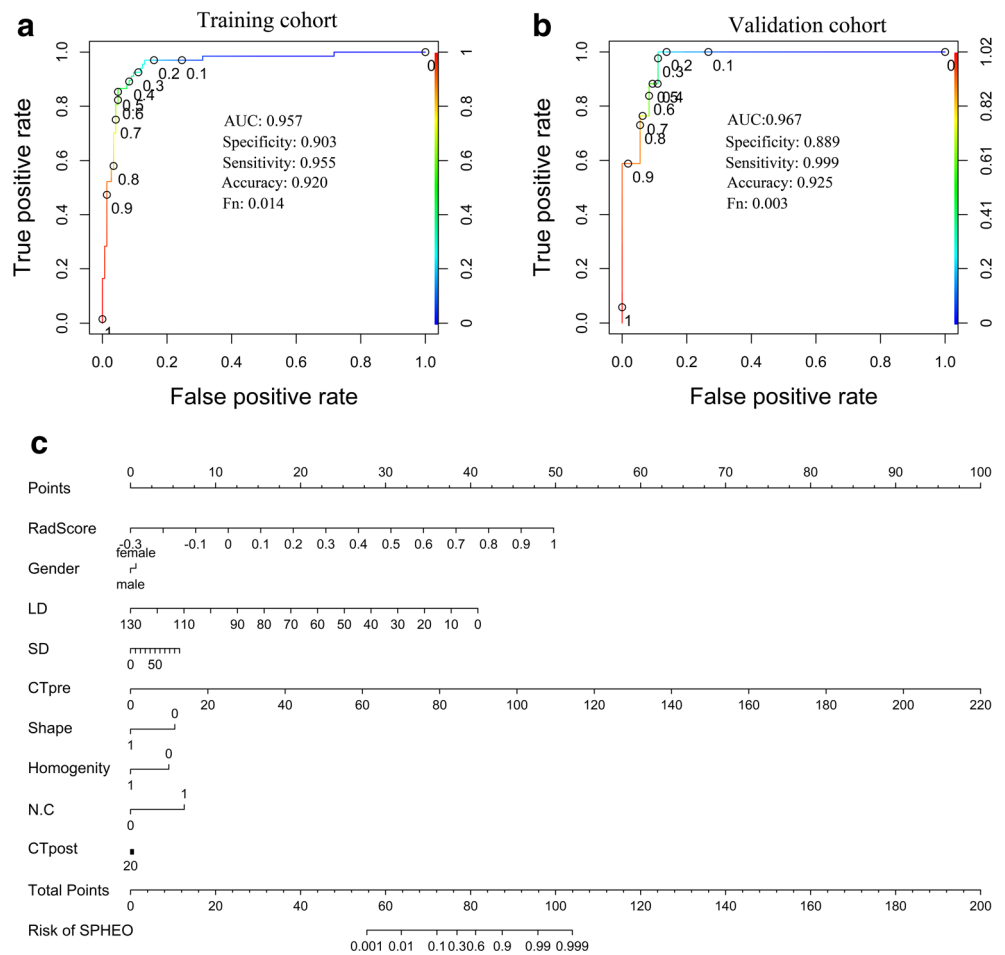
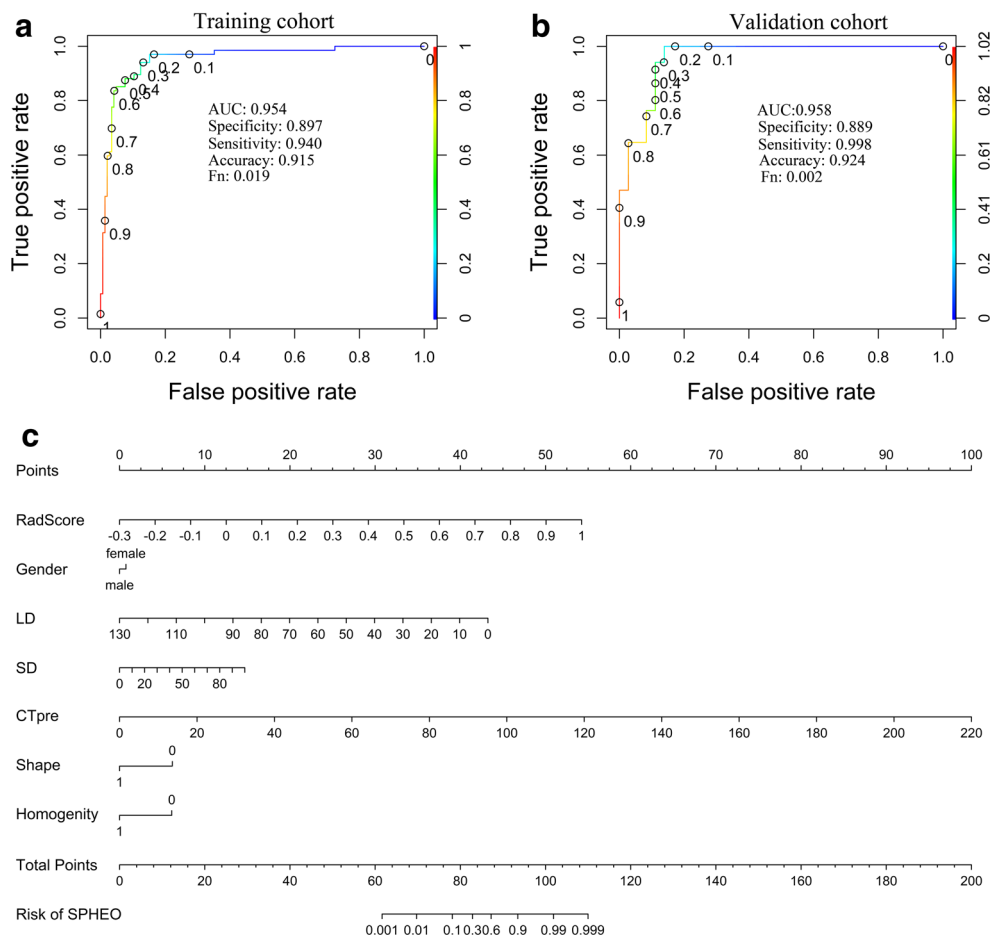


Fig. 4 Receiver operating characteristic (ROC) curves based on the nomogram without enhanced CT features (necrosis/cystic degeneration, N/C). Cut-off values are indicated along the curves. **a** ROC curve for the training cohort. **b** ROC curve for the validation cohort. **c** Nomogram without N/C



either enhanced or unenhanced images, are shown in Fig. S3. They both showed good agreement between evaluation by the radiomic nomogram and actual observation.

Discussion

Radiomics for medical imaging analysis facilitates identification of predictive diagnostic imaging biomarkers, which allows for a personalized approach to therapy [10]. Such information may help clinicians use a PPPM approach [1–3] to optimize presurgical diagnosis of subclinical pheochromocytoma. In the present study, we found that the Rad-score alone could differentiate sPHEO from LPA. Our predictive models combining the Rad-score with traditional imaging features improved performance in differentiating the sPHEO from LPA. Using AI as an example, our study showed the relevance of using a PPPM approach to predict the tumor pathology correctly before surgery, preventing any potential adverse outcomes during surgery and enabling a personalized therapeutic strategy for each patient.

Our study was designed to address a real dilemma that is encountered by clinicians, especially radiologists and

surgeons [7, 20]. In clinical practice, AIs are often identified when patients undergo a routine abdominal or chest CT scan, even when it is only a non-contrast CT scan. A dedicated multi-phase contrast-enhanced CT adrenal scan may help the radiologists to make a definitive diagnosis regarding the pathology of the tumor, but the potential risk of an additional CT scan should be considered. The disadvantages of doing a second scan include additional cost, radiation hazards and the potential risks associated with contrast media, which include allergy and potential renal damage. Unfortunately, the majority of patients currently undergo an additional CT scan due to the difficulty in distinguishing the various adrenal tumors with traditional radiological analysis. Furthermore, the risks associated with contrast media are further exacerbated in vulnerable populations such as the elderly and pediatric populations.

Our approach has some advantages over the existing methods in AI research filed. Our approach is part of a growing number of studies that use a new kind of predictive models for pre-operative diagnosis of cancer. For example, one study combined a large panel of predictors, including radiological and clinicopathological features, to improve the prediction of lymph node metastasis in colorectal cancer [21]. Notably, this method relied heavily on the key factors chosen to construct

the prediction model. In addition, in traditional predictive model studies, their method required many cases to achieve high efficiency (sensitivity and specificity), which was not practical. The number of patients enrolled in clinical studies is usually modest and therefore only a few features could be included, which may lead to decreased accuracy in predictive models. Our study overcame this issue by using Rad-score as a single key factor through data reduction method for modeling throughout the study. Therefore, the impact on accuracy of predictive modeling, which caused by the modest number of patients included in the study or the limited number of features should be included in the model building, seems to be overcome transiently in our study, as it would have if the previously published method was used [21]. In addition, our study introduces the Rad-score, which was calculated using 16 radiomic features selected by LASSO regression and showed good classification ability in the ROC test. Our study results indicated that the Rad-score might be a useful stand-alone diagnostic indicator.

Application of radiomic analysis has been increasing in medical imaging research [10, 22, 23]. Successful examples have been reported for cancers throughout the body [10, 22–25]. Radiomic models have been reported as potential biomarkers for distinguishing different types of tumors or different subtypes of a common tumor. Furthermore, radiomic signatures could be important predictors for differential diagnosis, therapeutic response, and survival in cancers [26, 27]. Most recently, radiomics has been used to differentiate small angiomyolipoma without visible fat from renal cell carcinoma with high accuracy, sensitivity, and specificity (93.9, 87.8, and 100%, respectively) [14]. Therefore, radiomic signatures can be useful in clinical practice.

Our study has filled a gap in the literature on sPHEO in the setting of AI. Previous studies on AIs have mostly focused on the differentiation of benign and malignant adrenal tumors. Prior studies have reported that some imaging characteristics on CT scans, as well as a dedicated adrenal CT scan with washout and 15-min delayed imaging, could be helpful in differentiating adenoma from other adrenal tumors [28–30]. However, specific data on LPA and sPHEO has been lacking. Gufler et al. reported an attempt to distinguish metastatic adrenal tumors from benign lesions, using 56 adrenal tumor cases with a history of malignancy [31]. The researchers developed a scoring system based on traditional radiological features in pre-enhanced CT images, which demonstrated a high efficiency for identifying metastatic lesions. Our study is similar to theirs in that both studies developed effective scoring systems for identifying adrenal tumors. However, our study focus was different; we studied benign adrenal tumors, and they studied both benign and malignant adrenal tumors. In addition, our study had the advantage of a large study cohort with all cases pathologically confirmed

while their study had a much smaller cohort with only a part of the cohort pathologically confirmed. To the best of our knowledge, our study presents the largest cohort to date for sPHEO and LPA in the setting of AI.

Our findings may have value for clinical practice. The goal of imaging for an adrenal tumor is to differentiate a lesion that may need treatment, such as pheochromocytoma, from a benign “leave-alone” tumor, such as an adenoma. From a radiological perspective, an optimal algorithm should be used to differentiate the leave-alone lesions from the lesions that need treatment using as few features as possible [28]. Our study has yielded very encouraging results. It is exciting that we may not need the additional contrast-enhanced adrenal CT scan. A non-contrast-enhanced CT scan is easier to obtain with reliable image quality, cheaper, and less time-consuming than enhanced CT or other imaging modalities such as magnetic resonance imaging (MRI) and positron emission tomography (PET)/CT. More importantly, the CT images already obtained for clinical purposes may be sufficient for clinicians to perform the calculations introduced in the present study. Therefore, our results may be rapidly incorporated into clinical practice.

There are several limitations to our study. First, due to the retrospective nature of the study, there might be selection bias. Second, the clinical outcome and prognosis data for the cardiology and oncology domains were not available due to lack of relevant documentation in the medical records or loss of follow-up clinical visits. Because of the benign nature of the adrenal tumors in this study, patients and their doctors do not have a strong incentive to follow-up after initial treatment. Third, we used a validation cohort that was from the same institution as the training cohort, which prevented us from generalizing the results to other institutions and other clinical settings. As a single-center study, the patient population was relatively small and homogeneous. A large-scale independent prospective multicenter study is needed to assess the generalizability of the results. Fourth, it is possible that adding features from other imaging modalities, such as MRI or PET/CT, might improve the accuracy of the model. However, this was beyond the scope of this study and will require further investigation. Fifth, although we only compared sPHEO and LPA in the present study, this method should be validated when adding other adrenal tumors with similar overlapping CT findings in future studies. Last, the radiomics features in our study were extracted from the largest cross-sectional area of the tumor. We recognize that different approaches, such as assessing the entire tumor in a three-dimensional image may provide additional information about tumor heterogeneity and may affect the study results. Nevertheless, our method of selecting the largest cross-sectional area of the tumor has been validated in previous published studies [21, 32].

Conclusions and expert recommendations

In conclusion, our PPPM-based radiomic models were effective in differentiating sPHEO from LPA in the setting of AI. In addition, our pre-enhanced CT-based nomogram has the advantage of avoiding the additional radiation exposure, risk, and cost of enhanced CT. The two models may allow clinicians to use existing pre-enhanced or enhanced CT images to correctly predict the pathology of adrenal tumors before surgery. Future prospective multicenter studies with larger samples may be needed to validate our models for clinical practice.

Our promising study result may facilitate PPPM-based efforts in both research and clinical practice. By assisting clinicians to make an accurate pre-operative diagnosis without additional imaging examination, the implementation of our diagnostic algorithm may improve personalized therapy. Moreover, we believe this CT image-based model and operational algorithm may be replicated by other institutions.

Based on our experience from the present study, we believe the following recommendations are important for establishing an accurate pre-operative diagnosis of adrenal tumors using PPPM principles [1–3]. First, multidisciplinary collaboration and partnership, including radiologists, urologists, cardiologists, and endocrinologists, are essential for the successful planning, calculation, integration, and applicability of radiomic research results in clinic practice. Second, quality CT images are vital for achieving an accurate diagnosis. These recommendations can enable the radiomics method developed here to improve predictive diagnostics and support personalized medicine.

Acknowledgements We thank Taihao Jin (Ph.D), from the Department of Diagnostic Radiology (City of Hope National Medical Center) for helpful discussion and assistance in preparing the manuscript. Editing assistance was provided by Nancy Linford, PhD.

Funding This study is partially supported in part by China Postdoctoral Science Foundation funded project (2018M632997) and The Postdoctoral Science Foundation of Central South University (No. 185705).

Compliance with ethical standards

Competing interests The authors declare that they have no competing interests.

Consent for publication Not applicable.

Ethical approval All procedures performed in studies involving human participants were in accordance with the ethical standards of the institutional and/or national research committee and with the 1964 Helsinki declaration and its later amendments or comparable ethical standards. For this type of study, formal consent is not required.

References

- Golubnitschaja O, Baban B, Boniolo G, Wang W, Bubnov R, Kapalla M, et al. Medicine in the early twenty-first century: paradigm and anticipation-EPMA position paper 2016. *EPMA J.* 2016;7(23):23. <https://doi.org/10.1186/s13167-016-0072-4>.
- Grech G, Zhan X, Yoo BC, Bubnov R, Hagan S, Danesi R, et al. EPMA position paper in cancer: current overview and future perspectives. *EPMA J.* 2015;6(9):9. <https://doi.org/10.1186/s13167-015-0030-6>.
- Golubnitschaja O, Costigliola V. General report and recommendations in predictive, preventive and personalised medicine 2012: white paper of the European Association for Predictive, Preventive and Personalised Medicine. *EPMA J.* 2012;3:14. <https://doi.org/10.1186/1878-5085-3-14>.
- Umanodan T, Fukukura Y, Kumagai Y, Shindo T, Nakajo M, Takumi K, et al. ADC histogram analysis for adrenal tumor histogram analysis of apparent diffusion coefficient in differentiating adrenal adenoma from pheochromocytoma. *J Magn Reson Imaging.* 2017;45:1195–203. <https://doi.org/10.1002/jmri.25452>.
- Park BK, Kim B, Ko K, Jeong SY, Kwon GY. Adrenal masses falsely diagnosed as adenomas on unenhanced and delayed contrast-enhanced computed tomography: pathological correlation. *Eur Radiol.* 2006;16:642–7. <https://doi.org/10.1007/s00330-005-0017-0>.
- Park BK, Kim CK, Kwon GY, Kim JH. Re-evaluation of pheochromocytomas on delayed contrast-enhanced CT: washout enhancement and other imaging features. *Eur Radiol.* 2007;17:2804–9. <https://doi.org/10.1007/s00330-007-0695-x>.
- Zhang Y, Cai P, Chen M, Yi X, Li L, Xiao D, et al. Imaging findings of adrenal primitive neuroectodermal tumors: a series of seven cases. *Clin Transl Oncol.* 2017;19:641–9. <https://doi.org/10.1007/s12094-016-1580-3>.
- Zhang YM, Lei PF, Chen MN, Lv XF, Ling YH, Cai PQ, et al. CT findings of adrenal schwannoma. *Clin Radiol.* 2016;71:464–70. <https://doi.org/10.1016/j.crad.2016.01.010>.
- Zhou Y, Tang Y, Tang J, Deng F, Gong G, Dai Y. Primary adrenal leiomyosarcoma: a case report and review of literature. *Int J Clin Exp Pathol.* 2015;8:4258–63.
- Lambin P, RTH L, Deist TM, Peerlings J, de Jong EEC, van Timmeren J, et al. Radiomics: the bridge between medical imaging and personalized medicine. *Nat Rev Clin Oncol.* 2017;14:749–62. <https://doi.org/10.1038/nrclinonc.2017.141>.
- Aerts HJ, Velazquez ER, Leijenaar RT, Parmar C, Grossmann P, Carvalho S, et al. Decoding tumour phenotype by noninvasive imaging using a quantitative radiomics approach. *Nat Commun.* 2014;5(4006):4006. <https://doi.org/10.1038/ncomms5006>.
- Goh V, Ganeshan B, Nathan P, Juttla JK, Vinayan A, Miles KA. Assessment of response to tyrosine kinase inhibitors in metastatic renal cell cancer: CT texture as a predictive biomarker. *Radiology.* 2011;261:165–71. <https://doi.org/10.1148/radiol.11110264>.
- Dennie C, Thornhill R, Sethi-Virmani V, Souza CA, Bayanati H, Gupta A, et al. Role of quantitative computed tomography texture analysis in the differentiation of primary lung cancer and granulomatous nodules. *Quant Imaging Med Surg.* 2016;6:6–15. <https://doi.org/10.3978/j.issn.2223-4292.2016.02.01>.
- Feng Z, Rong P, Cao P, Zhou Q, Zhu W, Yan Z, et al. Machine learning-based quantitative texture analysis of CT images of small renal masses: differentiation of angiomyolipoma without visible fat from renal cell carcinoma. *Eur Radiol.* 2017;28:1625–33. <https://doi.org/10.1007/s00330-017-5118-z>.
- Chang K, Bai HX, Zhou H, Su C, Bi WL, Agbodza E, et al. Residual convolutional neural network for the determination of IDH Status in low- and high-grade gliomas from MR imaging.

- Clin Cancer Res. 2017;24:1073–81. <https://doi.org/10.1158/1078-0432.CCR-17-2236>.
16. Birkhahn M, Mitra AP, Cote RJ. Molecular markers for bladder cancer: the road to a multimarker approach. *Expert Rev Anticancer Ther.* 2007;7:1717–27. <https://doi.org/10.1586/14737140.7.12.1717>.
 17. Croner RS, Förtsch T, Brückl WM, Rödel F, Rödel C, Papadopoulos T, et al. Molecular signature for lymphatic metastasis in colorectal carcinomas. *Ann Surg.* 2008;247:803–10. <https://doi.org/10.1097/SLA.0b013e31816bcd49>.
 18. Cheng T, Zhan X. Pattern recognition for predictive, preventive, and personalized medicine in cancer. *EPMA J.* 2017;8:51–60. <https://doi.org/10.1007/s13167-017-0083-9>.
 19. Szczypiński PM, Strzelecki M, Materka A, Klepaczko A. MaZda—a software package for image texture analysis. *Comput Methods Prog Biomed.* 2009;94:66–76. <https://doi.org/10.1016/j.cmpb.2008.08.005>.
 20. Yi X, Long X, Xiao D, Zai H, Li Y. Rhabdomyosarcoma in adrenal region of a child with hypertension and fever: a case report and literature review. *J Pediatr Surg.* 2013;48:e5–8. <https://doi.org/10.1016/j.jpedsurg.2013.01.018>.
 21. Huang YQ, Liang CH, He L, Tian J, Liang CS, Chen X, et al. Development and validation of a radiomics nomogram for preoperative prediction of lymph node metastasis in colorectal cancer. *J Clin Oncol.* 2016;34:2157–64. <https://doi.org/10.1200/JCO.2015.65.9128>.
 22. Limkin EJ, Sun R, Dercle L, Zacharaki EI, Robert C, Reuzé S, et al. Promises and challenges for the implementation of computational medical imaging (radiomics) in oncology. *Ann Oncol.* 2017;28:1191–206. <https://doi.org/10.1093/annonc/mdx034>.
 23. Gillies RJ, Kinahan PE, Hricak H. Radiomics: images are more than pictures, they are data. *Radiology.* 2016;278:563–77. <https://doi.org/10.1148/radiol.2015151169>.
 24. Zhang B, Tian J, Dong D, Gu D, Dong Y, Zhang L, et al. Radiomics features of multiparametric MRI as novel prognostic factors in advanced nasopharyngeal carcinoma. *Clin Cancer Res.* 2017;23:4259–69. <https://doi.org/10.1158/1078-0432.CCR-16-2910>.
 25. Zhang B, He X, Ouyang F, Gu D, Dong Y, Zhang L, et al. Radiomic machine-learning classifiers for prognostic biomarkers of advanced nasopharyngeal carcinoma. *Cancer Lett.* 2017;403:21–7. <https://doi.org/10.1016/j.canlet.2017.06.004>.
 26. Bogowicz M, Riesterer O, Ikenberg K, Stieb S, Moch H, Studer G, et al. Computed tomography radiomics predicts HPV status and local tumor control after definitive radiochemotherapy in head and neck squamous cell carcinoma. *Int J Radiat Oncol Biol Phys.* 2017;99:921–8. <https://doi.org/10.1016/j.ijrobp.2017.06.002>.
 27. Huang Y, Liu Z, He L, Chen X, Pan D, Ma Z, et al. Radiomics signature: a potential biomarker for the prediction of disease-free survival in early-stage (I or II) non-small cell lung cancer. *Radiology.* 2016;281:947–57. <https://doi.org/10.1148/radiol.2016152234>.
 28. Berland LL, Silverman SG, Gore RM, Mayo-Smith WW, Megibow AJ, Yee J, et al. Managing incidental findings on abdominal CT: white paper of the ACR incidental findings committee. *J Am Coll Radiol.* 2010;7:754–73. <https://doi.org/10.1016/j.jacr.2010.06.013>.
 29. Mendiratta-Lala M, Avram A, Turcu AF, Dunnick NR. Adrenal Imaging. *Endocrinol Metab Clin N Am.* 2017;46:741–59. <https://doi.org/10.1016/j.ecl.2017.04.009>.
 30. Boland GW, Blake MA, Hahn PF, Mayo-Smith WW. Incidental adrenal lesions: principles, techniques, and algorithms for imaging characterization. *Radiology.* 2008;249:756–75. <https://doi.org/10.1148/radiol.2493070976>.
 31. Gufler H, Eichner G, Grossmann A, Krentz H, Schulze CG, Sauer S, et al. Differentiation of adrenal adenomas from metastases with unenhanced computed tomography. *J Comput Assist Tomogr.* 2004;28:818–22.
 32. Feng Z, Rong P, Cao P, Zhou Q, Zhu W, Yan Z, et al. Machine learning-based quantitative texture analysis of CT images of small renal masses: differentiation of angiomyolipoma without visible fat from renal cell carcinoma. *Eur Radiol.* 2018;28:1625–33. <https://doi.org/10.1007/s00330-017-5118-z>.